Thermal properties of phosphate glasses for salt waste immobilization

Pawel Stoch · Malgorzata Ciecinska · Agata Stoch

Abstract Vitrification is the most effective method of the hazardous waste immobilization. Toxic elements are incorporated into glass structure. Iron phosphate glasses are presently being considered as a matrix for storage of the radioactive waste which cannot be vitrified using a conventional borosilicate glass. Influence of Na_2SO_4 as one of the components such the waste on thermal properties and crystallization ability of iron phosphate waste glass was studied. It was observed that Na_2SO_4 decreases transformation temperature and increases ΔC_p. The glass characteristic temperatures, glass crystallization ability, and crystallizing phases were determined. Na_2SO_4 increases the glass crystallization ability which could be related with ΔC_p heat capacity accompanying glass transition changes. The glass internal structure rebuilding, accompanying the sodium content increase, is considered. It is shown that ΔC_p is a suitable, structure-sensitive glass crystallization ability, parameter.

Keywords Iron phosphate glass · Thermal analysis · Thermal properties · Nuclear waste · Vitrification

P. Stoch (✉) · M. Ciecinska
Faculty of Material Science and Ceramics, AGH-University of Science and Technology, Mickiewicza 30 Ave., 30-059 Kraków, Poland
e-mail: pstoch@agh.edu.pl

A. Stoch
Institute of Electron Technology Krakow Division, Zablocie 39, 30-701 Kraków, Poland

Introduction

Vitrification is the most effective methods of the hazardous waste immobilization. Toxic elements are incorporated into glass structure. Borosilicate glasses are of common use in nuclear waste immobilization procedure. Lately, glasses from Fe_2O_3–P_2O_5 system are of the great interest, for scientific reason and because they are considered as a high-capacity matrix for storage of radioactive waste [1, 2]. The worldwide-used borosilicate glasses for nuclear waste vitrification are not suitable for immobilization of high-content molybdenum, chromium, or salt waste because of the low solubility of these compounds in the borosilicate glass Therefore, it is necessary to look for an alternate vitrification matrix. The next choice is the phosphate glasses. However, the most of phosphate glasses have a low chemical durability, but iron as a glass component significantly increases it. Among other phosphate glasses the highest chemical durability is reported for $60P_2O_5$–$40Fe_2O_3$ (Fe/P = 0.67) glass. All of them have O/P ratio over 0.3 and are classified as polyphosphate glasses [3]. It indicates that iron strengthens the chemical bonds in glass structure making their properties comparable or even better than borosilicate glasses [1, 2].

The iron phosphate glasses, besides their excellent chemical durability, have the melting temperature about 100–200 K lower than borosilicate glass, and due to the high fluidity of the melts, their homogenization time is about 1.5–3 h shorter [4]. It is way they can be suitable for vitrifying waste containing significant quantities of volatile elements such as Cs. Moreover, iron phosphate glasses exhibit particularly high thermal stability in terms of the low crystallization tendency and can be produced in big quantities without danger of crystallization matrix. Depending on the composition and heating schedule,

Table 1 Chemical composition of the glasses/mol%

Oxide	PFS0	PFS10	PFS20	PFS30	PFS50
P_2O_5	63	56	50	44	32
Fe_2O_3	37	34	30	26	18
Na_2SO_4		10	20	30	50

glassy materials could be obtained but often with crystalline particulate inclusions [1].

Use of the iron phosphate glasses for vitrification of waste which contains: relatively high concentration of actinide elements, high concentration of sodium, cesium sulfate, chloride-containing waste, chloride waste from pyrochemical reprocessing of Pu metal, waste containing various metals, radioactive ceramics, polymers, and carbon is now being considered [1, 5].

Taking all of these into account in the present paper, the influence of Na_2SO_4 as one of the salty waste components on the thermal properties, especially glass stability against crystallization of P_2O_5–Fe_2O_3 of constant Fe/P = 0.6 glass was studied. The structural aspects of the high capacity of salt waste incorporation are being considered as well.

Experimental

Glass containing 37 mol% Fe_2O_3 and 63 mol% P_2O_5 was prepared from chemically pure $NH_4H_2PO_4$ and Fe_2O_3. Batches were melted for 2 h at 1,373 K in Al_2O_3 crucible in an electric furnace with the furnace atmosphere as close to natural as possible. The melt was vitrified by casting onto steel plate and crushed into 0.3- to 0.1-mm grain size. The obtained glass frit was mixed with Na_2SO_4 (used as waste simulator) and remelted at 1,373 K for 2 h. Na_2SO_4 to the glass ratio was $x = 0$, 10, 20, 30, and 50 mass%. Samples were designated as PFS0, PFS10, PFS20, PFS30, and PFS50, respectively (Table 1).

Glass transformation temperature T_g at the half of the heat capacity step on DSC curve, crystallization T_C as the onset of the first crystallization peak, and melting T_M as the onset of the first melting peak temperatures were measured by differential scanning calorimetry (DSC) method at the heating rate of 10 K min^{-1}. Measurements were carried out using Perkin Elmer DTA/DSC/TG—seven heat flow differential scanning calorimeter. Pure Al and Au were used for temperature and heat calibration. Value of specific heat capacity change ΔC_p (J g^{-1} K^{-1}), accompanying glass transformation, was determined using Perkin Elmer Pyris Thermal Analysis Software Library program.

Crystallization of the glasses was checked by heating the powdered samples by 2 h at T_c temperature of exothermic DSC peak. Phase composition of the samples was
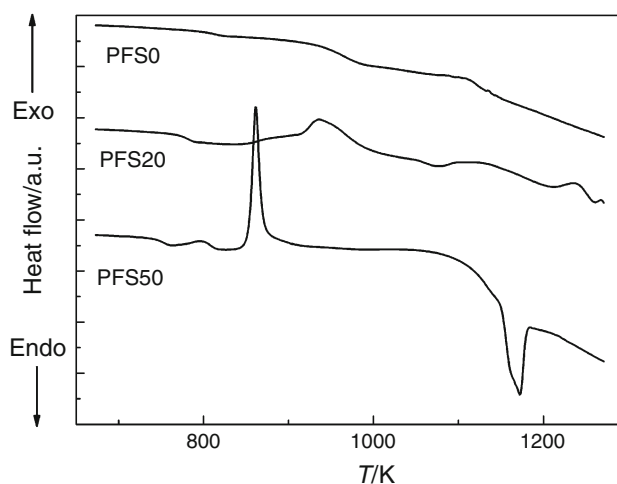
Fig. 1 DSC curves of the PFS0, PFS20, and PFS50 samples

Table 2 The transformation (T_g), crystallization (T_c), melting (T_m) temperatures, and ΔC_P, Hruby's parameter (K_H)
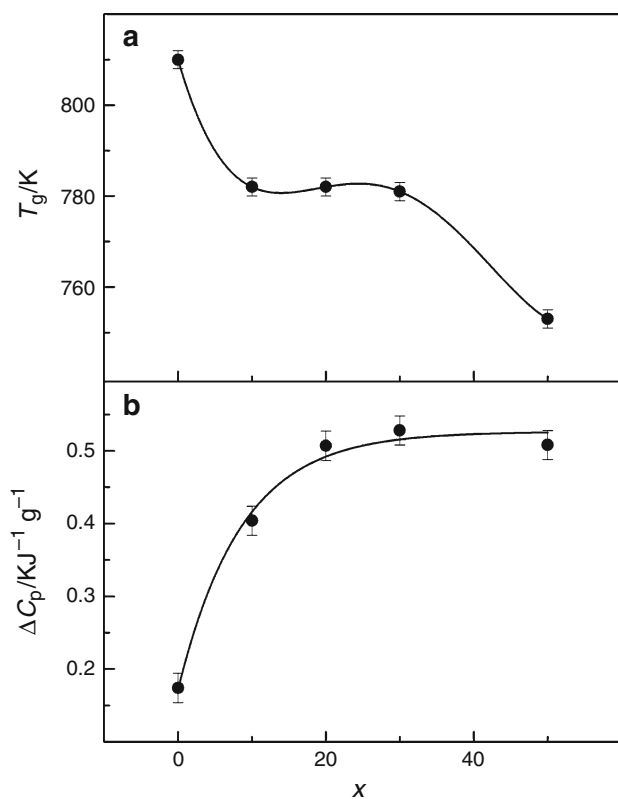
Sample	T_g/K	T_C/K	T_m/K	ΔC_P/J g^{-1} K^{-1}	K_H
PFS0	810 (2)	1,008 (2)	1,123 (2)	0.174 (9)	1.721
PFS10	782 (2)	967 (2)	1,192 (2)	0.404 (9)	0.822
PFS20	782 (2)	863 (2)	1,062 (2)	0.507 (9)	0.407
PFS30	781 (2)	873 (2)	1,123 (2)	0.528 (9)	0.368
PFS50	753 (2)	786 (2)	1,163 (2)	0.508 (9)	0.087

investigated by X-ray diffractometry (XRD) using DRON 1.5 apparatus, and Cu K$_\alpha$ radiation and the measured spectra were analyzed using X'Pert HighScore Plus software. The obtained spectra were fitted using Rietveld method, and semi-quantitative analysis of crystallizing phases was done.
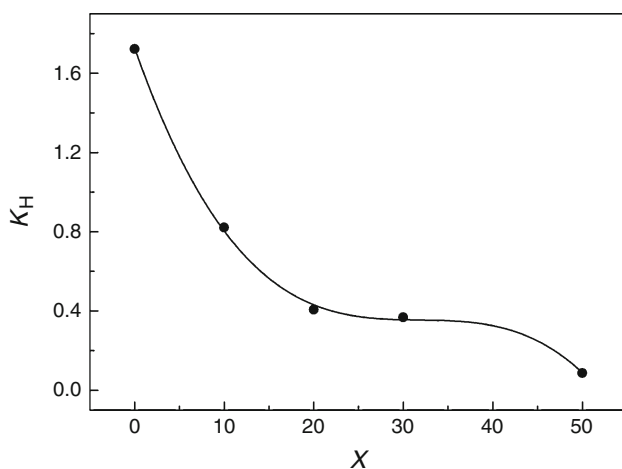
Glass density was measured by weightening of bulk glass samples in air and in water.

Results

The effect of addition of the Na_2SO_4 to the iron phosphate glass on its thermochemical properties is demonstrated by the DSC curves. An exemplary DSC curve for the base glass and the samples containing 20 and 50 mass% of sodium sulfate is presented in Fig. 1. All the samples show the transformation step which is increasing with Na_2SO_4 content and follow to the increase of the value of molar heat capacity change ΔC_p accompanying the glass transformation. Just behind, there appears an exothermic effect of crystallization, small and diffuse in the case of the base glass and stronger and stronger when sodium is added.
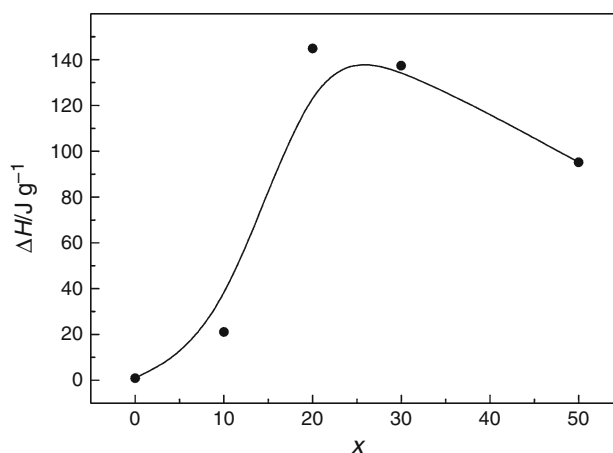
Fig. 2 Transformation temperature T_g (**a**) and the molar heat capacity ΔC_p accompanying the glass transformation (**b**) as function of the Na$_2$SO$_4$ addition (mol%)

Fig. 3 The Hruby parameter K_H as Na$_2$SO$_4$ content function

Fig. 4 Enthalpy of the crystallization of glasses (ΔH) as dependent on the Na$_2$SO$_4$ (mol%) content

accompanying the glass transformation is presented in Fig. 2. The T_g temperature is reduced with x increase; then, a kind of plateau appears (Fig. 2), and it persists almost constant upto about $x = 30$ than is dropping down again. The ΔC_p value is growing continuously with the sodium sulfate up to 30 mol% content (Fig. 2).

One of the important parameters in the case of waste vitrification is the thermal stability of the vitrified product. The glass stability of the investigated materials was evaluated using Hruby criterion. According to [6], the higher the K_H value the greater its stability against crystallization. The K_H value was evaluated according to the formulae:
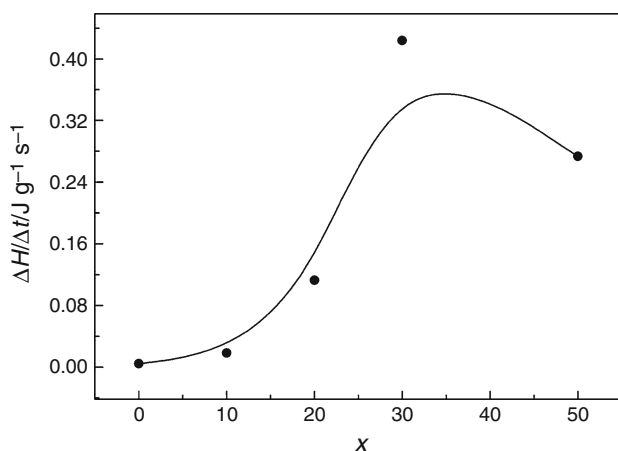
$$K_H = \frac{T_c - T_g}{T_m - T_c} \qquad (1)$$

The obtained K_H parameters are summarized in Table 2 and Fig. 3.
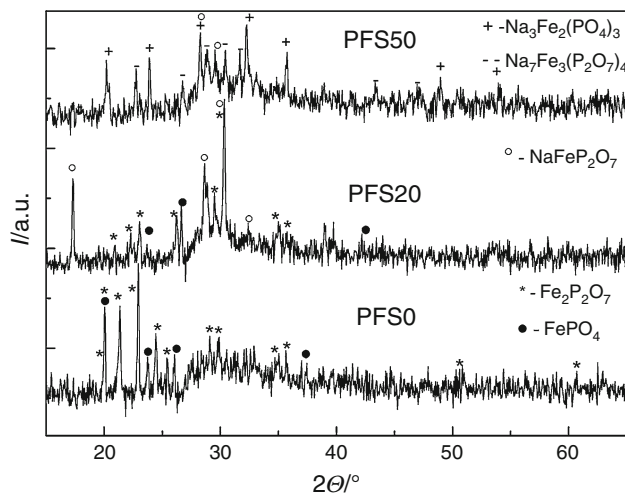
All of the investigated glasses except glass PFS50 evidenced good thermal stability comparable with conventional silicate glasses for which K_H value varied from 0.14 to about 1.3 [7–9]. The increasing Na$_2$SO$_4$ addition causes decrease of the K_H parameter which means lowering the glass stability against crystallization and at the same ability of glass to vitrify on cooling [9].

Enthalpy of crystallization calculated from DSC curves' exothermic peak area was taken as an arbitrary measure of the glass crystallization degree. Its value is growing up rapidly with Na$_2$SO$_4$ content but above $x = 30$ mol% is falling down (Fig. 4). Accordingly, the shape of DSC peak is changing (Fig. 1). It is more and more narrow and sharp, which indicates the change of crystallization kinetics.

To quantify this observation, the ratio $\Delta H/\Delta t$ was taken as crystallization factor. It is changing at the range of 20–30 mol% Na$_2$SO$_4$ content (Fig. 5). This suggests the change of the crystallization mechanism above the Na$_2$SO$_4$ 20 mol% content.

After crystallization effect, melting of the glass occurs. The similar curves are observed for the rest of the measured samples. The transformation, crystallization, and melting temperatures of the investigated materials are presented in Table 2.

Influence of the Na$_2$SO$_4$ content on transformation temperature T_g and the molar heat capacity ΔC_p

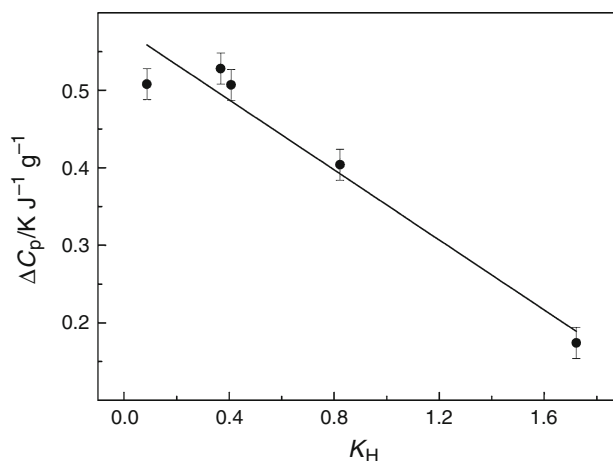Fig. 5 Kinetics crystallization factor $\Delta H/\Delta t$ change with Na_2SO_4 content (mol%)

Fig. 6 XRD patterns of compounds crystallizing in the PFS0, PFS20, and PFS50 glasses

Table 3 Compounds crystallizing in the investigated glasses, semi quantity analysis, and ICDD reference codes

Sample	Crystal phase	Semi quantity/mass%	Ref. code
PFS0	$FePO_4$	30	00-050-1635
	$Fe_2P_2O_7$	70	01-072-1516
PFS10	$FePO_4$	10	00-050-1635
	$Fe_2P_2O_7$	40	01-072-1516
	$NaFeP_2O_7$	50	01-076-1762
PFS20	$FePO_4$	5	00-050-1635
	$Fe_2P_2O_7$	25	01-072-1516
	$NaFeP_2O_7$	70	01-076-1762
PFS30	$FePO_4$	3	00-050-1635
	$NaFeP_2O_7$	52	01-076-1762
	$Na_3Fe_2(PO_4)_3$	45	00-045-0319
PFS50	$NaFeP_2O_7$	22	01-076-1762
	$Na_3Fe_2(PO_4)_3$	49°	00-045-0319
	$Na_7Fe_3(P_2O_7)_4$	29	00-049-1129

Fig. 7 Dependence of the molar heat capacity ΔC_p change versus the K_H parameter

The XRD patterns of the compounds crystallizing in PFS0, PFS20, and PFS50 glasses at Tc temperature indicated by the DSC are presented in Fig. 6 and Table 3. The main crystalline phases formed in the base glass (PFS0) are iron phosphates $FePO_4$ and $Fe_2^{II}(P_2O_7)_2$. Addition of sodium besides iron phosphate results in the formation of the sodium containing compounds as $NaFe^{III}P_2O_7$. Further increasing of sodium concentration leads to crystallization of $Na_3Fe_2^{III}(PO_4)_3$ which crystallizes at cost of the iron phosphates. For the glass PFS50, there is no evidence of crystallization of $FePO_4$ or $Fe_2^{3+}Fe^{2+}(P_2O_7)_2$ but formation of sodium-rich phases, like $Na_3Fe_2(PO_4)_3$ and $Na_7Fe_3(P_2O_7)_4$, is detected. Generally, in iron phosphate glasses, composition of the crystallizing compounds depends on the glass composition, heat treatment and its atmosphere, and the Fe^{2+}/Fe^{3+} ratio. Phases formed in the

glasses investigated here are similar to those observed in the case of crystallization cesium iron phosphate glasses [10, 11].

The Na_2SO_4 incorporation leads to growth of Na_2O content and increases the change of the specific heat capacity ΔC_p accompanying the glass transformation (Fig. 2b). As was mentioned previously [12, 13], ΔC_p value can be the indicator of a degree of the structural changes accompanying the transformation, like number and strength of the broken bonds and rearrangement of structure constituents.

Results of the measurements proved the relation between ΔC_p and the K_H values which could describe glass stability against crystallization (Fig. 7). As can be clearly visible, the higher the ΔC_p value means the lower the glass
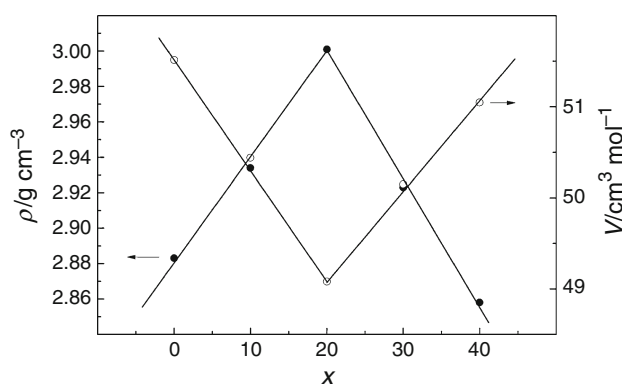
Fig. 8 Density (*black circles*) and molar volume (*open circles*) as Na$_2$SO$_4$ content

stability and in the same way the lower the K_H parameter. This proves that the ΔC_p value obtained by DSC method, could be used also as glass stability against crystallization parameter. The ΔC_p value is related to the change of entropy accompanying glass transition and at the same as the structure rebuilding degree indicator [14].

The glass densities and molecular volumes accompanying them are presented in Fig. 8. As can be clearly seen, the glass density increases up to $x = 20$ and for higher Na$_2$SO$_4$ content is decreasing. The molar volume behaves in the opposite way.

Discussion

Iron belongs to the group of metallic elements B, Al, and Fe which in their three valent state possess an ability to form specific phosphate glasses of composition corresponding to orthophosphates BPO$_4$, AlPO$_4$, and FePO$_4$. They distinguish the higher chemical durability and thermal stability, as compared to glasses containing these elements but having lower metal (Me) to phosphorous Me/P ratio. Structure and properties of the orthophosphate glasses are not recognized good enough, specially the iron phosphate glasses.

The most information can be found about AlPO$_4$ glass and its crystalline analog berlinite. Berlinite structure is close to the structure of quartz (SiO$_2$) framework silicate, but instead of [SiO$_4$] tetrahedra it is built of [AlO$_4$][PO$_4$] groups, geometrically, and crystallochemically equivalent to [SiO$_4$][SiO$_4$] pair. Similarity is so close that berlinite like quartz has tridymite- and cristobalite-like polymorphic modifications. It is also generally supposed that AlPO$_4$ glass has the vitreous SiO$_2$-like structure. Silica glass (*v*-SiO$_2$) structure accepts some quantities of AlPO$_4$ and mixed network glass, chemically durable and high-temperature resistant is formed.

The BPO$_4$ exhibits analogous similarity to SiO$_2$ structure and dissolves in vitreous silica. As it was demonstrated earlier, BPO$_4$–SiO$_2$ glass dissolves considerable quantities of AlPO$_4$ and three component AlPO$_4$–BPO$_4$–SiO$_2$ glass with polymeric mixed network is formed [15]. NMR studies of this glass proved that in its structure, 2/3 Al^{3+} has coordination number (*CN*) 4 and B^{3+} cation possesses the same coordination. This indicates that structure of the glass consists of [AlO$_4$], [BO$_4$], and [SiO$_4$] tetrahedra, joined together by oxide bridges. It means that all of them play the same function in the structure of glass, as network-formers. Addition of Na$_2$O in the quantities higher than 10 mol% changes the *CN* of part of three valent cations in structure, and [AlO$_6$] and [BO$_3$] polyhedra appear. Their number increases with Na$_2$O content [15].

In the chain structure of metaphosphate Na$_2$O–Al$_2$O$_3$–P$_2$O$_5$ glasses, Al^{3+} has *CN* 6 and together with Na$^+$ alternatively saturates the charge of the non-bridging oxygen in the phosphate chains. Similar Al and Na arrangements appear in pyrophosphate glasses from this system. In the orthophosphate glass structure [PO$_4$], tetrahedron is saturated by two Al^{3+} ions with the *CN* 4 and one with *CN* 6 and plus one cation Na$^+$. With the Al$_2$O$_3$ content increase, the content of alumina in coordination 4 and orthophosphate [PO$_4$] groups increase accordingly [16]. When the ratio Al$_2$O$_3$/P$_2$O$_5$ exceeds 0.63, glass network is made up mainly by the [AlO$_4$] and [PO$_4$] tetrahedra, joined each other by the bridging oxygen's—mixed alumino-phosphate network [17].

Iron orthophosphate FePO$_4$ possesses many similarities to berlinite, and it has also iron tridymite and iron cristobalite modifications, which indicates the structural similarity of both of the compounds.

However, according to investigations of local iron environment in phosphate glass 40Fe$_2$O$_3$–60P$_2$O$_5$ (mol%) melted at varying temperatures and under different atmospheric conditions, it contains both Fe^{III} and Fe^{II} ions [18]. The average iron–oxygen coordination is 4–5 and iron ions have mixed tetrahedral–octahedral coordination and Fe^{3+} ions occupy two distinct sites in glass structure.

Existence of FeO$_5$ instead of FeO$_6$ polyhedra for Fe^{II} and FeO$_6$ octahedra for Fe^{3+} in the glass of ultraphosphate composition ware was suggested in [19]. On the other hand, Mössbauer spectroscopy study of the SiO$_2$–P$_2$O$_5$–Al$_2$O$_3$–Fe$_2$O$_3$–CaO containing different, up to 14.8, mass% of Fe$_2$O$_3$ [22] indicates that coordination number of iron cations depends on Fe^{2+} to the total Fe content ratio. For glasses synthesized in oxidizing condition, iron in both Fe^{2+} and Fe^{3+} state exists predominantly in tetrahedral coordination. In more reduced conditions, glass abundance of tetrahedrally coordinated Fe^{3+} decreases linearly with increasing Fe^{2+} content.

Basic glass investigated here contains 63 mol% P$_2$O$_5$ and 37 mol% Fe$_2$O$_3$ and Fe/P ratio is equal to 0.6, which

corresponds the polyphosphate compounds which have chain and ring phosphate groups in the structure. To saturate free phosphate charges in such a structure, the valence of part of Fe^{3+} has to be reduced to Fe^{2+}. High melting temperature of the glass and excess of phosphate groups in melts promote the Fe^{3+} reduction. To completely saturate the phosphate charges, the melt should contain 27 mol% orthophosphate $Fe^{III}[PO_4]$ groups and 73 mol% of chains of $Fe^{II}[P_2O_7]$.

The XRD pattern demonstrated that both of these phosphates crystallize in the glass, heat-treated (Table 3), and quantitative proportions of them are close to calculated above. As it was demonstrated in [20, 21], between T_g and liquid temperature, at the viscoelastic state of glass, its crystallization proceeds by successive ordering and diffusional growth of local groups of atoms, forming middle range order clusters. The basic glass crystallization was carried out in DSC-measured temperature which is close to T_g and much lower than melting temperature (Table 1). This suggests that basic glass structure contains polymerized $Fe[PO_4]$ groups, phosphate chains, and/or pyrophosphate pairs of phosphate tetrahedral $[P_2O_7]^{4-}$.

According to XRD results, Na_2SO_4 incorporation into the basic glass changes its physical properties, which is accompanied by internal structure rebuilding. This is evidenced by the composition of compounds crystallizing in glass. Sodium oxide increases the oxygen content in structure of glass, promoting oxidation of Fe^{2+} and Fe^{3+} content increase. Moreover, Na^+ participates in the saturation of phosphate charges and Na, Fe-phosphates crystallize in glass. In 10 mol% Na_2SO_4-containing glass, this is $NaFeP_2O_7$ and its number is growing up. When it reaches 50 mol%, compounds $NaFeP_2O_7$, $Na_3Fe_2(PO_4)_3$, and $Na_7Fe_3(P_2O_7)_4$ are crystallizing (Table 3).

Addition of Na_2O to the basic glass increases the metallic cations to phosphorus Na + Fe/P ratio from 0.6 in basic glass to 2.1 for PFS50 sample. Change in structure of the glasses is a result of this as well. In oxide glasses, Na^+ breaks the oxide bridges, disintegrating the network. Part of Fe–O–P bonds is broken and substituted by $Na–PO_4$ bonds, and number of this substitution is growing with sodium content. Formulas of compounds crystallizing in glasses (Table 3) are the argument for this. The substitution degree expressed by Na/Fe^{III} ratio is growing in them, it needs, in parallel progressive decomposition of phosphate network, into pyrophosphate elements and finally, when Na + Fe/P exceeds 2.0, into separate $[PO_4]$ tetrahedra (PFS50 glass). The latest glass has chemical formula $1.6Na_2O·0.6Fe_2O_3·P_2O_5$, which means that its structure consists of pyro- and ortho-phosphate groups surrounded by Na^+ and Fe^{3+} cations. Accordingly, molecular volume (V) of glass changes with Na_2O content increase. At the beginning, its value is going down which is demonstrated by the structure density increase and next is growing up (Fig. 8). Content of 20 mol% of Na_2SO_4 and Na + Fe/P > 1 is the turning point of molecular volume vs sodium oxide (x) content relation. Structure densification can be explained as an effect of the increase of Fe^{3+} content being the effect of oxidizing action of Na_2O and stabilizing three valent iron existence. Moreover, Na^+ is breaking part of P–O–P bridges and small pyrophosphate groups, surrounded by Fe^{3+} plus Na^+ are formed. Smaller network-forming P_2O_5 groups surrounded by Na^+ and joined with them by undirectional ionic bonds make the structure flexible. This leads to possibility of the glass structure components to change their positions according to the chemical minimum free energy rule.

Further, Na_2O content increases, above the turning point, when Na + Fe/P ratio exceeds 1, resulting in molar volume increase (Fig. 8). This can be explained as disintegration of phosphate network groups, up to separate $[PO_4]$ tetrahedral formation. Mechanism of the structure rebuilding, proposed here, has support in the chemical composition of compounds crystallizing in glass (Table 3). It explains also the change of thermal properties of glass as Na_2SO_4 content dependent (x).

The Na_2SO_4 incorporation increases the change of the specific heat capacity ΔC_p accompanying the glass transformation (Fig. 2b). As was mentioned previously [12, 13], ΔC_p value can be the indicator of configuration entropy increase as dependent on degree of the structure organization changes, accompanying the transformation, like number of the broken bonds and forms of existence and arrangement of constituents of structure. As it was mentioned above, sodium into glass structure breaks network oxide bridges, reducing their number and separating network into smaller, at the same more mobile species. Accordingly in structure, the number of undirectional ionic Na–O bonds increases. All of these make the glass structure more flexible and easier to reorganize which can be deeper and deeper with x value increase, and explains ΔC_p increase, accompanying T_g decrease (Fig. 2a).

Curve of the T_g vs x value relation is dropping down rapidly at the beginning but near the turning point $x = 20$ mol%, it stabilizes and characteristic plateau appears (Fig. 2a). It is accompanied by change of slope of the curve of ΔC_p of glass transformation (Fig. 2b). This indicates that first stage of structure rebuilding is a source of the relatively high change of heat capacity, suggesting the deep structure reorganization. It can be a consequence of the iron oxidation and number of Fe–O–P bridges linking phosphate group increase and structure of glass stabilization. Above the turning point at Na_2O 20 mol%, further increase of ΔC_p is incomparably smaller, which means the smaller differences in the elements of structure composition and distribution, as it was suggested above.

Increasing molar volume value together with diminishing number of Fe as phosphate group joining component, and increasing Na in composition of the crystallizing compounds, suggests diminishing number of the Fe–O–P cross-linking bridges and weakening structure of glass. Properly, glass crystallization is easier and easier, and its temperature and at the same, thermal glass stability parameter K_H glass are lowering (Fig. 7). On the other hand, crystallization degree, measured by heat of DSC exothermic peak area, is increasing (Fig. 4). The crystallization peak becomes narrow and sharp (Fig. 4), which means the change of crystallization kinetics from slow to very fast, due to increasing mobility and easer rearrangement of elements in the structure, when concentration of sodium is increasing (Fig. 5).

Generally, results of the investigation of the thermal properties of Fe_2O_3–P_2O_5 glass did not confirm the earlier supposition on octahedral coordination of both Fe^{2+} and Fe^{3+} being the result of spectroscopic measurement interpretation [18, 19].

Phosphate glasses exhibit a nonlinearity of change the properties with their chemical composition change. The rapid change of the function of phosphate glass property versus composition is termed the phosphate anomaly, by analogy to the commonly-known boron or alumina anomaly connected with the change in their coordination number 4–6 and transition of the cation from network former to modifier position. The phosphate anomaly is an effect of the structure rebuilding, under the change of the proportions of components content, as for example, transition from ultra- to poly- to pyro- and/or ortho-phosphate condensation state accompanied by diminishing the number of the surrounding bridging oxides Q_n, from Q_3 to Q_0. The investigation of the thermal properties of iron phosphate glasses proved that they also exhibit phosphate anomaly effect. This peculiarity explains the large capacity of incorporation of salt waste as Na_2SO_4 of the Fe_2O_3–P_2O_5 glasses.

Conclusions

Thermal properties of $37Fe_2O_3$–$63P_2O_5$ (mol%) glass, with increasing content of Na_2O added to it as Na_2SO_4, being the simulator of the radioactive salt waste, were investigated. It was demonstrated that the change of the properties with the glass chemical composition change exhibits a nonlinearity, being the effect of internal structure rebuilding, accompanying the sodium content increase.

The phosphate glasses exhibit effect of the structure rebuilding, under the components content proportion change, as transition from ultra- to poly- to pyro- and/or ortho-phosphate condensation state accompanied by diminishing the number of the surrounding bridging oxides Q_n, from Q_3 to Q_0,

termed phosphate anomaly. The investigation of the thermal properties of iron phosphate glasses proved that they also exhibit the phosphate anomaly effect accompanied by structure expansion and molar volume increase. This peculiarity explains the big capacity of the Fe_2O_3–P_2O_5 glasses for incorporation of salt waste as Na_2SO_4.

References

1. Donald W. Immobilisation of radioactive and non-radioactive wastes in glass-based systems: an overview. Glass Technol. 2007;48:155–63.
2. Ojovan MI, Lee WE. An introduction to nuclear waste immobilisation. Amsterdam: Elsevier Science; 2005.
3. Brow RK. Review: the structure of simple phosphate glasses. J Non-Cryst Solids. 2000;263, 264:1–28.
4. Kim CW, Day DE. Immobilization of Hanford LAW in iron phosphate glasses. J Non-Cryst Solids. 2003;331:20–31.
5. Bingham PA, Hand RJ, Scales CR. Immobilisation of simulated plutonium-contaminated material in phosphate glasses: an initial scoping study. Mater Res Soc Symp Proc. 2006;932:345–52.
6. Hruby A. Evaluation of glass-forming tendency by means of DTA. Czech J Phys B. 1972;22:1187–96.
7. Cabral AA, Cardoso AAD, Zanotto ED. Glass-forming ability versus stability of silicate glasses I. Experimental test. J Non-Cryst Solids. 2003;320:1–8.
8. Lin SE, Cheng YR, Wei WCJ. Synthesis and long-term test of borosilicate-based sealing glass for solid oxide fuel cells. J Eur Ceram Soc. 2011;31:1975–85.
9. Nascimento MLF, Souza LA, Ferreira EB, Zanotto ED. Can glass stability parameters infer glass forming ability? J Non-Cryst Solids. 2005;351:3296–308.
10. Joseph K, Ghosh S, Govindan Kutty KV, Vasudeva Rao PR. Crystallization kinetics, stability and glass forming ability of iron phosphate and cesium loaded iron phosphate glasses. J Nucl Mater. 2012;426:223–39.
11. Biningham PA, Barney ER. Structure of iron phosphate glasses modified by alkali and alkaline earth additions: neutron and X-ray diffraction studies. J Phys. 2012;24:175403–16.
12. Stoch L, Wacławska I, Środa M. Thermal study of the influence of chemical bond iconicity on the glass transformation in (Na_2O, CaO, MgO)–Al_2O_3–SiO_2 glasses. J Therm Anal Calorim. 2004;77:57–63.
13. Stoch L. Thermochemistry of solids with flexible structures. J Therm Anal Calorim. 1998;54:9–24.
14. Stoch L. Thermal analysis and thermochemistry of vitreous to crystalline state transition. J Therm Anal Calorim. 2004;77:7–16.
15. Stoch L, Sroda M, Olejniczak Z. Synthesis and structure of $AlPO_4$–BPO_4–SiO_2 glasses, ceramics, Polish Ceramic Bulletin, Polish Academy of Science, Krakow. 1997;15:119–128.

16. Brow RK. The nature of alumina in phosphate glass I. Properties of sodium aluminophosphate glass. J Am Ceram Soc. 1993;76: 913–8.

17. Jin Y, Jiang D, Chen X, Bian B, Huawy X. Raman spectrum studies of the glasses in the system $Na_2O–Al_2O_3–P_2O_5$. J Non-Cryst Solids. 1986;80:147–51.

18. Karabulut M, et al. An investigation of the local iron environment in iron phosphate glasses having different Fe(II) concentrations. J Non-Cryst Solids. 2002;306:182–92.

19. Hoppe U, Karabut M, Metwalli E, Brow RK, Jovari P. The Fe–O coordination in phosphate glasses by X-ray diffraction with high energy photons. J Phys. 2003;15:6143–53.

20. Stoch L, Stoch P. Crystal structures formation in glass from view of HRTEM. J Therm Anal Calorim. 2007;88:577–82.

21. Stoch L, Stoch P. Significance of crystallochemical factors in chemical reactions into the structure of solids. J Therm Anal Calorim. 2012;109:763–6.

22. Hannant OM, Bingham PA, Hand RJ, Forder SD. The structural properties of iron in vitrified waste ashes, glass technology. J Glass Sci Technol. 2008;49:27–32.